Acta Crystallographica Section F
Structural Biology and Crystallization Communications
ISSN 1744-3091

Veerendra Kumar, Nagarajan Mallika and J. Sivaraman*

Department of Biological Sciences, National University of Singapore, 14 Science Drive 4, Singapore 117543, Republic of Singapore

Correspondence e-mail: dbsjayar@nus.edu.sg

Received 3 June 2011
Accepted 5 August 2011

Purification, crystallization and diffraction studies of the methyltransferases BT_2972 and BVU_3255 from antibiotic-resistant pathogens of the genus *Bacteroides* from the human intestine

The methyltransferases BT_2972 and BVU_3255 from two different *Bacteroides* species that are antibiotic-resistant pathogens from the human intestine were cloned, overexpressed and purified, yielding approximately 120 mg of each protein from 1 l culture. Apo BT_2972 and BVU_3255 and their complexes with *S*-adenosylmethionine or *S*-adenosylhomocysteine were crystallized in four different crystal forms using the hanging-drop vapour-diffusion method. These crystals diffracted to resolutions ranging from 2.8 to 2.2 Å. Sequence analysis suggested that the two proteins are homologous small-molecule methyltransferases.

1. Introduction

Methyltransferases are key regulatory enzymes that catalyze the transfer of a methyl group from *S*-adenosylmethionine (SAM; the donor molecule) to a variety of acceptor molecules (substrates) such as DNA, RNA, proteins, lipids or small molecules (Martin & McMillan, 2002). The SAM-dependent methyltransferases (class I methyltransferases) consist of a seven-stranded β-sheet flanked by three α-helices on both sides (Schubert *et al.*, 2003) and are also known as Rossmann-fold methyltransferases (RFMs; Bujnicki, 1999). Most of the macromolecular methyltransferases are found to contain two separate domains, one each for substrate binding and SAM binding, while the small-molecule methyltransferases have substrate-binding and SAM-binding sites within the same domain. In addition, the small-molecule methyltransferases have two additional α-helices at the N-terminus (Martin & McMillan, 2002).

The adult human intestine is dominated by bacteria of the genus *Bacteroides*. *Bacteroides* generally live in a symbiotic relationship, but they have also been found to be opportunistic pathogens (McCarthy *et al.*, 1988). *Bacteroides* bacteria show resistance towards various antibiotics such as clindamycin, chloramphenicol, carbenicillin, lincomycin and tetracycline (Bodner *et al.*, 1972). Recently, the complete genomes of two species, *B. thetaiotaomicron* VPI-5482 and *B. vulgatus* ATCC 8482, of the genus *Bacteroides* have been sequenced (Xu *et al.*, 2003, 2007). An open reading frame (ORF) in the chromosomal genome of *B. thetaiotaomicron* VPI-5482 encodes a putative methyltransferase BT_2972 (accession No. NP_811884). Similarly, BVU_3255 (accession No. YP_001300506) is a putative methyltransferase from *B. vulgatus* ATCC 8482. To the extent of our understanding, BT_2972 and BVU_3255 have not yet been shown to confer any antibiotic resistance. Previously, apo structures of BT_2972 (PDB entry 3f4k) and BVU_3255 (PDB entry 3e7p) and the structure of the closely related protein complex Q5LES9_BACFN–SAM from *B. fragilis* NCTC 9343 (PDB entry 3kkz) have been determined by the Northeast Structural Genomics Consortium and the New York SGX Research Center for Structural Genomics but have not yet been reported in the literature. Towards understanding the structure and function of these two homologous methyltransferases (which have 59% sequence identity), we here report the cloning, protein expression and biophysical characterization of BT_2972 and BVU_3255. Both proteins were crystallized in the apo form and as complexes with ligands such as SAM and *S*-adenosylhomocysteine (SAH). Sequence analysis suggests that both BT_2972 and BVU_3255 are

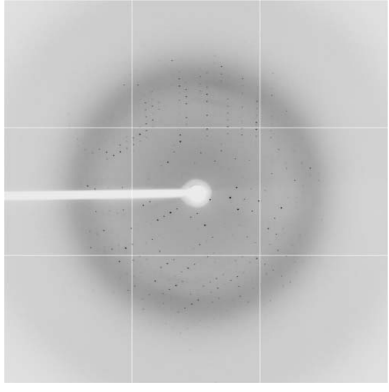

Table 1
Crystallization conditions and data-collection statistics.

Values in parentheses are for the highest resolution bin.

	BT_2972			BVU_3255		
	Native	SAM	SAH	Native	SAM	SAH
Crystallization conditions	0.12 *M* magnesium acetate, 16% PEG 3350	25%(*v*/*v*) 2-propanol, 0.1 *M* MES monohydrate pH 6.0, 18%(*w*/*v*) PEG MME 2000	25%(*v*/*v*) 2-propanol, 0.1 *M* MES monohydrate pH 6.0, 18%(*w*/*v*) PEG MME 2000	170 m*M* magnesium acetate, 15% PEG 3350	150 m*M* ammonium chloride, 17%(*w*/*v*) PEG 3350, 3%(*v*/*v*) 2-propanol	120 m*M* ammonium nitrate, 16%(*w*/*v*) PEG 3350. 200 m*M* nondetergent sulfobetaine 221
Unit-cell parameters (Å, °)	*a* = 60.55, *b* = 74.38, *c* = 117.11	*a* = 120.79, *b* = 59.68, *c* = 77.62, β = 104.61	*a* = 60.64, *b* = 74.52, *c* = 117.22	*a* = 132.06, *b* = 72.14, *c* = 55.90	*a* = 73.42, *b* = 106.65, *c* = 133.0	*a* = 73.98, *b* = 107.05, *c* = 133.10
Space group	$P2_12_12_1$	*C*2	$P2_12_12_1$	$P2_12_12$	$P2_12_12_1$	$P2_12_12_1$
No. of molecules in the asymmetric unit	2	2	2	2	4	4
Matthews coefficient V_M (Å^3 Da^{-1})	2.20	2.26	2.21	2.22	2.17	2.20
Solvent content (%)	44.1	45.5	44.3	44.6	43.4	44.0
Resolution range (Å)	50.0–2.80 (2.90–2.80)	50.0–2.40 (2.49–2.40)	50.0–2.30 (2.38–2.30)	50.0–2.90 (3.00–2.90)	50.0–2.20 (2.28–2.20)	50.0–2.49 (2.53–2.49)
Wavelength (Å)	1.5418	1.0000	1.0000	1.5418	1.000	1.5418
Oscillation angle (°)	1	1	1	1	1	1
No. of images	360	180	120	360	150	360
Observed reflections	108383	63495	82597	64399	258707	276109
Unique reflections	13019 (1002)	20044 (1537)	22841 (2040)	11578 (902)	50893 (3594)	36997 (1884)
Multiplicity	8.3 (3.4)	3.2 (2.4)	3.6 (2.6)	5.6 (2.7)	5.1 (4.4)	7.5 (5.3)
Completeness (%)	95.3 (74.7)	94.7 (73.1)	93.5 (86.0)	92.8 (74.5)	94.7 (68.0)	95.6 (91.4)
$\langle I/\sigma(I)\rangle$	4.1 (2.0)	9.9 (2.6)	10.2 (2.3)	23.3 (4.7)	15.0 (7.5)	15.4 (4.4)
R_{merge}†	0.110 (0.185)	0.059 (0.200)	0.074 (0.215)	0.105 (0.18)	0.055 (0.24)	0.091 (0.52)

† $R_{merge} = \sum_{hkl}\sum_i |I_i(hkl) - \langle I(hkl)\rangle| / \sum_{hkl}\sum_i I_i(hkl)$, where $I_i(hkl)$ is the intensity of the ith measurement of reflection hkl and $\langle I(hkl)\rangle$ is the mean intensity for that reflection.

small-molecule methyltransferases and are involved in the methylation of intermediates in the ubiquinone-biosynthesis pathway.

2. Materials and methods

2.1. Cloning

Genes encoding BT_2972 (gene ID 1075985) and BVU_3255 (gene ID 5304216) were chemically synthesized (GeneScript, USA) and inserted into pUC57 cloning vector. Subsequently, to clone them into the expression vector, these genes were further PCR-amplified from the respective pUC57 vector using the following primers: 5′-CTTTCATATGCATCATCATCATCATCATAGTAACAATAATACAT-3′ (forward) and 5′-CTTTCTCGAGTCATCTTTTTTGTCCTATATAGAATACGTA-3′ (reverse) for BT_2972 and 5′-CTTTCATATGCATCATCATCATCATAATAATGAC-3′ (forward) and 5′-CTTTCTCGAGTCACCTTCTCAGTGAGAATCC-3′ (reverse) for BVU_3255. This PCR amplification introduced *Nde*I and *Xho*I restriction sites at the 5′ and 3′ ends of each gene, respectively. This also resulted in the introduction of a Met start codon followed by a six-His codon at the 5′ end of each gene. Both PCR products were gel purified and then digested with *Nde*I and *Xho*I (NEB, England) along with vector pGS21a (GeneScript, USA). The digested gene products were ligated with pGS21a vector and transformed into *Escherichia coli* DH5α cells. Positive colonies were selected based on colony PCR and the sequence of the insert was verified by DNA sequencing.

2.2. Expression and purification

For large-scale protein expression, recombinant plasmids pGS21a-BT_2972 and pGS21a-BVU_3255 were transformed into chemically competent *E. coli* BL21 (DE3) cells. A single colony was chosen to inoculate 100 ml Luria Broth (LB) medium containing 100 µg ml^{-1} ampicillin and this was incubated overnight at 310 K with continuous shaking. 50 ml of this overnight-grown culture was used to inoculate 1 l LB medium, which was allowed to grow at 310 K until the OD_{600} reached 0.6–0.8. The culture was then induced with 0.15 m*M* IPTG and allowed to grow for a further 16 h at 289 K. The cells were harvested by centrifugation at 9800*g* for 10 min.

The cell pellets were resuspended in 100 ml lysis buffer composed of 50 m*M* Tris–HCl pH 7.4, 500 m*M* NaCl, 10%(*v*/*v*) glycerol, 20 m*M* imidazole and 20 m*M* β-mercaptoethanol. The cell suspension was sonicated for 5 min at 28% amplitude with 1 s on/1 s off pulses in a Vibra-Cell VCX750 ultrasonic processor using a 13 mm probe (Sonics). The cell lysate was centrifuged at 39 000*g* for 30 min at 277 K to remove cell debris and insoluble protein. The clear supernatant was mixed with 5 ml Ni–NTA resin (Qiagen) pre-equilibrated in lysis buffer and allowed to bind at 277 K for 2 h. After binding, the supernatant was removed and the Ni–NTA resin was washed three times using 10 ml lysis buffer each time with 15 min intervals. After washing, the bound proteins were released from Ni–NTA beads using lysis buffer supplemented with 300 m*M* imidazole. In the next step of purification, the BT_2972 and BVU_3255 fractions collected from Ni–NTA beads were passed through a gel-filtration column (HiLoad 16/60 Superdex 200 prep grade; Amersham Biosciences, Sweden). The column was pre-equilibrated with a buffer consisting of 20 m*M* Tris–HCl pH 7.4 and 200 m*M* NaCl. Gel-filtration chromatography was performed at 277 K using an ÄKTA FPLC. Protein quantification was performed by the Bradford method (Zor & Selinger, 1996) using reagents from Bio-Rad (USA).

2.3. Dynamic light scattering

Fractions of individual proteins from the gel-filtration chromatography were pooled together and concentrated to 10 mg ml^{-1}. The homogeneity of each of the concentrated proteins was checked by dynamic light scattering (DLS) using a DynaPro instrument (Protein Solutions, USA). All samples were centrifuged at 10 000*g* for 20 min before the experiment. The measurements were carried out at 298 K. The software provided by the manufacturer was used to calculate the hydrodynamic properties of BT_2972 and BVU_3255.

2.4. Crystallization

BT_2972 or BVU_3255 at a concentration of 10 mg ml^{-1} was mixed with SAM or SAH in a 1:5 protein:ligand ratio, which is well above the micromolar binding affinity indicated by preliminary calorimetry experiments (results not shown) for the formation of their respective complexes. The proteins and SAM/SAH were kept in a buffer consisting of 20 m*M* Tris–HCl pH 7.4 and 200 m*M* NaCl. Crystallization trials were performed for the apo proteins and the SAM and SAH complexes of both proteins. Crystallization experiments were performed manually using the hanging-drop vapour-diffusion method at room temperature. Typically, 1 µl protein solution and 1 µl reservoir solution were mixed together and equilibrated against 500 µl reservoir solution. Initial crystallization conditions were identified using the PEG/Ion and PEGRx 2 screens (Hampton Research). These conditions were optimized in order to obtain diffraction-quality crystals.

2.5. Data collection

Crystals of the proteins and their SAM or SAH complexes were soaked briefly (30 s) in a cryoprotectant solution consisting of mother liquor supplemented with 10%(*v*/*v*) glycerol, picked up in a nylon loop and flash-cooled at 100 K in an N_2 cold stream (McFerrin & Snell, 2002). Complete diffraction data sets for the apo-protein crystals were collected using a Bruker AXS X8 Proteum X-ray system (Bruker AXS Inc., Madison, USA), while those for the SAM–protein and SAH–protein complex crystals were collected on beamline X-12B1 (Quantum 4 CCD detector; Area Detector Systems Corp., Poway, California, USA) at the National Synchrotron Radiation Research Centre (NSRRC), Taiwan. The data-collection strategy is provided in Table 1. The data sets were processed using *HKL*-2000 (Otwinowski & Minor, 1997).

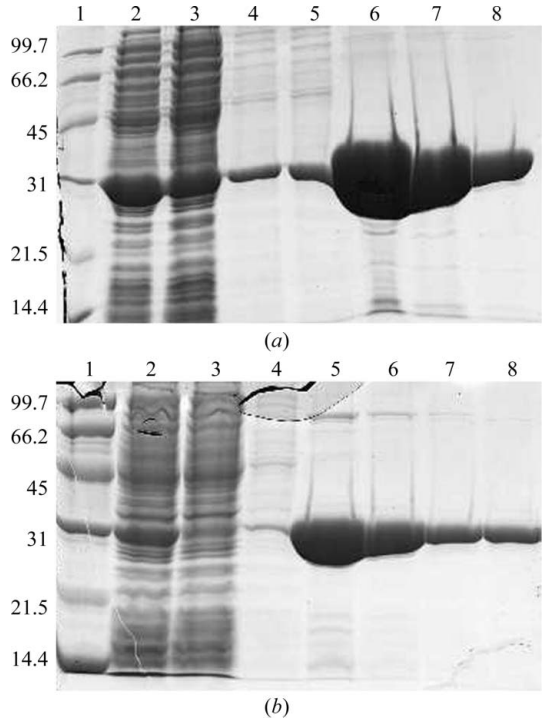

Figure 1
SDS–PAGE showing the expression and purification profiles of BT_2972 (*a*) and BVU_3255 (*b*). Lane 1, molecular-weight marker (labelled in kDa); lane 2, cleared lysate; lane 3, flowthrough after affinity binding; lanes 4 and 5, washes of Ni–NTA beads; lanes 6 and 7, elution from Ni–NTA beads; lane 8, gel-filtration fraction. Affinity-purified protein was overloaded in lane 6 in order to check for traces of impurities.

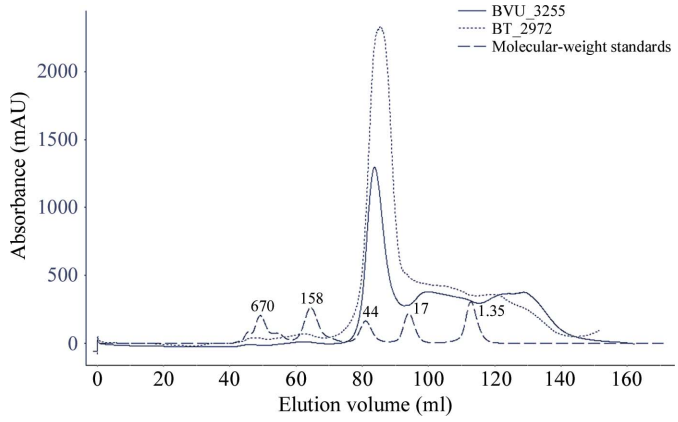

Figure 2
Gel-filtration chromatography elution profiles of BT_2972 (dotted line) and BVU_3255 (solid line). The elution profile of molecular-weight standards is shown as a dashed line and is marked with the different sizes of the proteins (kDa). The gel-filtration profile shows that both proteins elute as monomers.

3. Results

The optimized expression of BT_2972 and BVU_3255 from the pGS21a vector gave high yields and resulted in approximately 200 mg of each protein in the supernatant from 1 l cell culture (Figs. 1*a* and 1*b*). The BT_2972 and BVU_3255 proteins were purified by two chromatographic steps: Ni–NTA affinity chromatography followed by gel filtration. Both proteins eluted at a volume which corresponded to the monomer of the protein, as compared with molecular-weight standards (Fig. 2). The final yield of each of the purified proteins was approximately 120 mg per litre of culture and showed 99% purity on SDS–PAGE. The purified proteins were concentrated to 10 mg ml^{-1}. The size homogeneity of the proteins was monitored by dynamic light-scattering experiments (Supplementary Fig. 1[1]) during concentration and prior to crystallization, which showed that the molecular weights correspond to those of monomers in solution and are consistent with the gel-filtration observations.

Additionally, the identity of the purified proteins BT_2972 and BVU_3255 was verified by peptide mass fingerprinting (PMF) experiments (data not shown). In both the proteins PMF detected peptides from the C-terminus and Ni–NTA binding indicated the presence of a His tag at the N-terminus. This suggests that there was no proteolytic cleavage of the N- and C-termini.

The uncleaved His-tagged proteins were used for crystallization. Crystals appeared after 2 d and were grown for up to 7 d; they belonged to different space groups. The collected data sets were processed to the maximum possible resolution with acceptable multiplicity, completeness and $R_{\rm merge}$ in the highest resolution bin (Fig. 3 and Table 1). $V_{\rm M}$ calculations indicated the presence of two molecules in the asymmetric unit of apo BT_2972, its SAM and SAH complexes and apo BVU_3255, whereas four molecules were present in the asymmetric unit of BVU_3255 complexed with SAM or SAH. This was further confirmed by self-rotation function calculations. Notably, while we were in the data-collection stage, apo structures of both BT_2972 (PDB entry 3f4k) and BVU_3255 (PDB entry 3e7p)

[1] Supplementary material has been deposited in the IUCr electronic archive (Reference: HC5139).

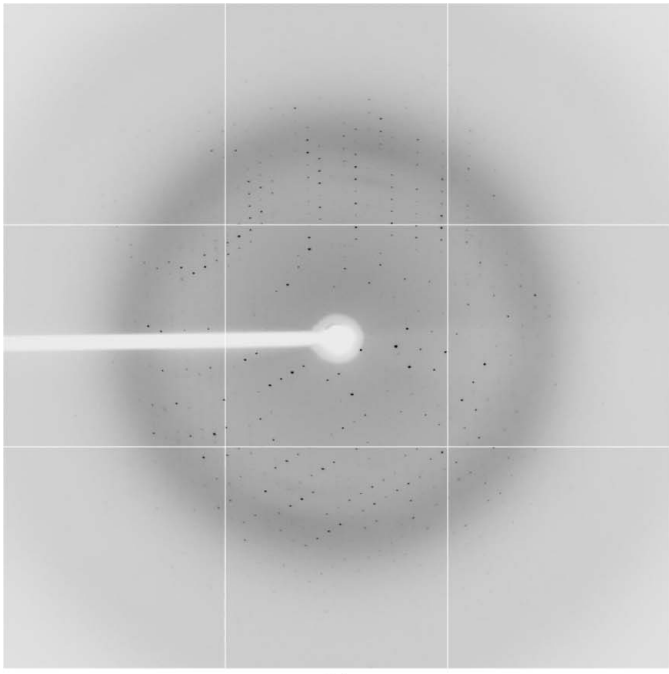

(*a*)

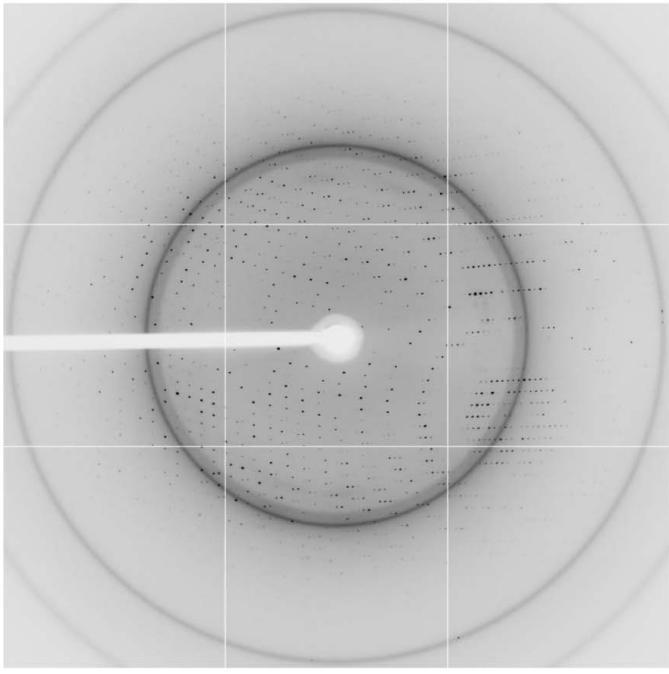

(*b*)

Figure 3
Representative diffraction patterns of crystals of BT_2972–SAM (*a*) and BVU_3255–SAH (*b*).

became available in the PDB; these structures had one molecule in the asymmetric unit.

Our BT_2972 structures (apo and SAM and SAH complexes) and PDB entry 3f4k belonged to three different space groups. In the case of BVU_3255 all three of our structures and PDB entry 3e7p belonged to different orthorhombic space groups. Our structures belonged to space groups $P2_12_12$ (apo) and $P2_12_12_1$ (SAM and SAH complexes), whereas PDB entry 3e7p belonged to space group $I222$. Similarly, a closely related SAM-dependent methyltransferase from *B. fragilis* crystallized (in complex with SAM) in space group $C2$ (PDB code 3kkz). The structures of both proteins and their complexes were determined by the molecular-replacement method using the program *MOLREP* in the *CCP*4 suite (Vagin & Teplyakov, 2010; Winn *et al.*, 2011). The structure solution clearly indicated the expected numbers of molecules in the asymmetric unit of BT_2972 and BVU_3255, with initial R factors in the range 0.39–0.42. The models were refined using *CNS* (Brünger *et al.*, 1998). The noncrystallographic symmetry (NCS) was used during the refinement. When the R factors were close to 0.30 the difference maps were calculated and clearly showed the presence of the ligands.

The *PISA* server (Krissinel & Henrick, 2007) showed that the symmetry-related molecules of 3f4k and 3e7p can form dimers, with a complexation score of 1. All the BT_2972 crystals and the apo BVU_3255 crystals showed two molecules in the asymmetric unit, with a similar dimer-interface region as predicted for 3f4k and 3e7p. Similarly, the SAM and SAH complexes of BVU_3255, with four molecules in the asymmetric unit, have a similar dimer-interface region. The observed common dimer interface suggests that the dimerization might be biologically relevant.

In summary, we have reported the expression, purification, crystallization (of apo protein as well as SAM and SAH complexes), data collection and diffraction analysis of the methyltransferases BT_2972 and BVU_3255. These studies led to the determination of the first representative structures of methyltransferases from the respective *Bacteroides* bacteria in complex with SAM or SAH. Sequence analysis of these two proteins suggest that they are homologous, with similar SAM/SAH-binding regions, and are small-molecule methyltransferases that are involved in the methylation of intermediates in the ubiquinone-biosynthesis pathway.

This work was supported by the Biomedical Research Council of Singapore (BMRC; R154000362305). VK is the recipient of a graduate scholarship from the National University of Singapore (NUS).

References

Bodner, S. J., Koenig, M. G., Treanor, L. L. & Goodman, J. S. (1972). *Antimicrob. Agents Chemother.* **2**, 57–60.
Brünger, A. T., Adams, P. D., Clore, G. M., DeLano, W. L., Gros, P., Grosse-Kunstleve, R. W., Jiang, J.-S., Kuszewski, J., Nilges, M., Pannu, N. S., Read, R. J., Rice, L. M., Simonson, T. & Warren, G. L. (1998). *Acta Cryst.* D**54**, 905–921.
Bujnicki, J. M. (1999). *In Silico Biol.* **1**, 175–182.
Krissinel, E. & Henrick, K. (2007). *J. Mol. Biol.* **372**, 774–797.
Martin, J. L. & McMillan, F. M. (2002). *Curr. Opin. Struct. Biol.* **12**, 783–793.
McCarthy, R. E., Pajeau, M. & Salyers, A. A. (1988). *Appl. Environ. Microbiol.* **54**, 1911–1916.
McFerrin, M. B. & Snell, E. H. (2002). *J. Appl. Cryst.* **35**, 538–545.
Otwinowski, Z. & Minor, W. (1997). *Methods Enzymol.* **276**, 307–326.
Schubert, H. L., Blumenthal, R. M. & Cheng, X. (2003). *Trends Biochem. Sci.* **28**, 329–335.
Vagin, A. & Teplyakov, A. (2010). *Acta Cryst.* D**66**, 22–25.
Winn, M. D. *et al.* (2011). *Acta Cryst.* D**67**, 235–242.
Xu, J., Bjursell, M. K., Himrod, J., Deng, S., Carmichael, L. K., Chiang, H. C., Hooper, L. V. & Gordon, J. I. (2003). *Science*, **299**, 2074–2076.
Xu, J. *et al.* (2007). *PLoS Biol.* **5**, e156.
Zor, T. & Selinger, Z. (1996). *Anal. Biochem.* **236**, 302–308.